QUERY FORM

MI	
Manuscript ID	**MI-16-261.R1 [Art. Id: mi201736]**
Author	Antonio Recchiuti
Editor	
Publisher	

Journal: MI

Author :- The following queries have arisen during the editing of your manuscript. Please answer queries by making the requisite corrections at the appropriate positions in the text.

Query No.	Description	Author's Response
GQ1	Please check Figures 1, 2, 3, 4, 5, 6, 7, 8 for accuracy as they have been relabelled.	Figures have been checked
GQ	Author surnames have been highlighted - please check these carefully and indicate if the first name or surname have been marked up incorrectly. Please note that this will affect indexing of your article, such as in PubMed.	Authors' surnames have been highlighted correctly.
Q1	Affiliations have been reordered for chronology. Please confirm.	Confirm
Q2	Please provide publisher name and place of publication in the reference 39.	Publisher name and place have been added to the proof
Q3	The symbol ** and *** is mentioned in the Figure 8 legend but is not present in the figure. Please indicate its position in the figure or delete.	The symbol ** and *** have been deleted. Sorry for the inconvenience

Resolvin D1 enhances the resolution of lung inflammation caused by long-term *Pseudomonas aeruginosa* infection

M Codagnone[1,2], E Cianci[1,2], A Lamolinara[2,3], VC Mari[2], A Nespoli[2,3], E Isopi[1,2], D Mattoscio[1,2], M Arita[4], A Bragonzi[5], M Iezzi[2,3], M Romano[1,2] and A Recchiuti[1,2]

Pseudomonas aeruginosa **lung infection is a main cause of disability and mortality worldwide. Acute inflammation and its timely resolution are crucial for ensuring bacterial clearance and limiting tissue damage. Here, we investigated protective actions of resolvin (Rv) D1 in lung infection induced by the RP73 clinical strain of *P. aeruginosa*. RvD1 significantly diminished bacterial growth and neutrophil infiltration during acute pneumonia caused by RP73. Inoculum of RP73, immobilized in agar beads, resulted in persistent lung infection up to 21 days, leading to a non resolving inflammation reminiscent of human pathology. RvD1 significantly reduced bacterial titer, leukocyte infiltration, and lung tissue damage. In murine lung macrophages sorted during *P. aeruginosa* chronic infection, RvD1 regulated the expression of Toll-like receptors, downstream genes, and microRNA (miR)-21 and 155, resulting in reduced inflammatory signaling. *In vitro*, RvD1 enhanced phagocytosis of *P. aeruginosa* by neutrophils and macrophages, recapitulating its *in vivo* actions. These results unveil protective functions and mechanisms of action of RvD1 in acute and chronic *P. aeruginosa* pneumonia, providing evidence for its potent pro-resolution and tissue protective properties on airway mucosal tissue during infection.**

INTRODUCTION

Pseudomonas aeruginosa is a major opportunistic pathogen that can cause a wide range of nosocomial infections with fatal outcome in immunocompromised or hospitalized patients. It is also the etiologic agent of chronic airway infections in patients with cystic fibrosis, bronchiectasis, and chronic bronchitis. Antibiotics are rarely successful, due to the intrinsic and acquirable resistance mechanisms exploited by *P. aeruginosa*.[1] In the United States, >6,000 healthcare-associated infections due to multi-drug resistant *P. aeruginosa* strains are reported every year.[2] In Europe, up to 50% of clinical isolates in 2014 were resistant to at least one antibiotic class (including β lactams, aminoglycosides, and fluoroquinolones) and ~14% of strains were found resistant to >3 antimicrobials.[3] In addition, *P. aeruginosa* exploits adaptation mechanisms to escape killing by the immune system and establish chronic infections that do not resolve.[4–6] Hence, both US and European health surveillance agencies classify *P. aeruginosa* as a "serious threat", emphasizing the urgent need for new strategies to combat its infections, limit the consequent exacerbated inflammation without immune suppression, and promote resolution.[2,3]

Pioneer work from Serhan and colleagues has demonstrated that resolution, the ideal outcome of acute inflammation,[7] is an active process controlled by endogenous specialized proresolving lipid mediators (SPM), i.e., Lipoxins (LX),[8] resolvins (Rv),[9,10] protectins (PD)[11] and maresins (Mar)[12] that are locally produced from polyunsaturated fatty acids in select phases of inflammation and resolution.[13] Established SPM bioactions encompass the ability to limit excessive leukocyte infiltration and responses to pathogens without immune-suppression, stimulate the removal of microbes and apoptotic cells via monocyte/macrophages (MΦs) phagocytosis, and protect the

[1]Department of Medical, Oral, and Biotechnology Science, University of Chieti-Pescara, Chieti, Italy. [2]Center on Aging Science and Translational Medicine (CeSI-MeT) "G. d'Annunzio", University of Chieti-Pescara, Chieti, Italy. [3]Department of Medicine and Aging Science, University of Chieti-Pescara, Chieti, Italy. [4]RIKEN Center for Integrative Medical Sciences, Kanagawa, Japan and [5]Infection and Cystic Fibrosis Unit, Division of Immunology, transplantation, and Infectious Diseases, IRCCS San Raffaele Scientific Institute, Milan, Italy. Correspondence: A Recchiuti (a.recchiuti@unich.it)

Received 12 September 2016; accepted 14 March 2017; doi:10.1038/mi.2017.36

host from collateral tissue damage.[14] Accruing evidence signifies that SPM have potent host-protective and proresolutive bioactions in experimental inflammatory diseases, including asthma,[15] arthritis[16] and infections[17–23] (see ref. 24 for a recent review), unveiling new strategies for the pharmacotherapy of human pathologies in light of the safety and effectiveness demonstrated by SPM in preclinical and initial clinical studies.[14,25,26]

Resolvin D1 (7S, 8R, 17S-trihydroxy-4Z, 9E, 11E, 13Z, 15E, 19Z –docosahexaenoic acid (DHA)) is an endogenous SPM enzymatically biosynthesized from DHA via lipoxygenases (LO).[27,28] It binds 2 specific GPCRs, ALX/FPR2 and GPR32/DRV1 to trigger cell-specific responses aimed at limiting excessive inflammation and stimulating return to homeostasis.[23] RvD1 stops polymorphonuclear neutrophil (PMN)-endothelial cell interactions and recruitment at sites of inflammation,[29] regulates specific MΦ microRNAs (miR) that control the release of inflammatory cytokines/chemokines and lipid mediators,[30,31] and stimulates MΦ phagocytosis,[18,32,33] polarizing these cells towards a pro-resolutive phenotype.[34] *In vivo*, RvD1 promotes resolution of allergen[35] or LPS[36] -induced airway inflammation and enhances bacterial killing during acute peritonitis, skin infection, and sepsis.[18,19] Thus, its role in *P. aeruginosa* lung infections is of wide interest.

Here, we demonstrate host-directed anti-microbial, anti-inflammatory, and pro-resolutive actions of RvD1 in acute and chronic lung infection triggered by a multi-drug resistant clinical strain of *P. aeruginosa.*

RESULTS

Lung inflammation associated with *P. aeruginosa* infection is markedly reduced by RvD1

To determine RvD1 actions on inflammation and bacterial clearance in preclinical models of *P. aeruginosa* lung infection reminiscent of human pathology, it was important to establish the temporal evolution of self-limited versus long-term lung infection with the clinical strain of *P. aeruginosa* RP73. Following intratracheal (i.t.) instillation of a planktonic suspension of RP73 cells ($\sim 1 \times 10^6$ CFU), the bacterial titer raised up to $\sim 6.0 \times 10^6$ CFU/lung 1 day post infection (DPI), decreased to $\sim 4.0 \times 10^5$ CFU/lung by 3 DPI, and further dropped to $< 10^1$ CFU/lung 7 DPI (**Figure 1a**) demonstrating bacterial clearance. Total leukocytes and PMN in BAL also rapidly increased 1 DP1 returning to normal by 7 days (**Figures 1b** and **c**), whereas monocytes and MΦs gradually increased and equaled PMN at 5 DPI, indicating resolution of inflammation. To better define resolution of acute *P. aeruginosa* pneumonia, we calculated mathematical resolution indices as defined by Bannenberg *et al*:[13] (a) Ψ_{max} = maximum PMN number ($\sim 3.4 \times 10^6$ cells/lung); (b) Ψ_{50} = 50% reduction in PMN ($\sim 1.7 \times 10^6$ cells/lung); (c) T_{max} = time when Ψ_{max} was reached ($\sim$1 DPI); (d) T_{50} = time of 50% in PMN ($\sim$ 2 DPI); (e) Resolution interval (R_i) = $T_{50} - T_{max}$, namely the time required for resolution; (f) $T_{PMN = Mono/M\Phi}$ = point of intersection of PMN and monocyte + MΦ numbers (**Figure 1c**).

In sharp contrast, the inoculum of RP73 cells embedded in agar beads, which allows bacteria to survive in the host airways for a long time by growing in a microaerobic/anaerobic environment, as in the mucus of chronically infected patients,[4,37] caused a high-titer infection (up to ~ 1–2×10^7 CFU/lung at 5 DPI) and produced a stable colonization ($\sim 1 \times 10^6$ CFU/lung) up to 21 days (**Figure 1a**), in keeping with recent results.[38] This was accompanied by a steep decline in body weight in the first 3 DPI that was followed by a gradual recover during the late infection phase (**Figure 1d**). A persistent significant accumulation of total leukocyte, PMN, and monocytes/MΦs in BAL was also evident up to 21 DPI (**Figures 1e and f**). Histological analysis revealed massive infiltration of PMN and lymphocytes in bronchial, peribronchial, alveolar and parenchymal areas in infected mice, whereas only sparse MΦs were present in lungs of uninfected animals. Metaplasia of mucous secretory cells (MuSC) was also detected, as indicated by the presence of PAS^+ cells in lung sections at 21 DPI, but not in uninfected controls (**Figure 1g**).

To characterize the soluble components of inflammation during chronic *P. aeruginosa* infection, lipidometabolomics and proteomics analyses were carried out. As shown (**Figure 1h** and **Table 1**), leukotriene (LT) B_4, and LTD_4 were markedly elevated at early phases (i.e. 5 DPI) of infection, while prostaglandin (PG) E_2 and other prostanoids involved in chronic inflammation were higher at 21 DPI. Of interest, several SPM (including RvD1), were below the lowest detection

Figure 1 Distinct outcomes of self-limited versus non resolving *P. aeruginosa* lung infection. (**a**) Number of living bacteria in BAL and lungs from mice infected with $\sim 3.5 \times 10^6$ CFU/mouse of planktonic or agar-embedded RP73. Total airway bacterial load was determined as the sum of the CFU found in BAL and lung suspensions upon serial dilution, spreading onto TSA, and o.n. growth. (**b**, **c**) Total and differential leukocyte counts in BAL from infected mice. **c** shows mathematical resolution indices: Ψ_{max}, maximum PMN number; T_{max}, time of Ψ_{max}; Ψ_{50}, 50% decrease in PMN number; T_{50}, time for Ψ_{50}; R_i, resolution interval (T_{50}–T_{max}); $T_{PMN = Mono/M\Phi}$, time of equivalence of PMN and monocytes/MΦ. (**d**) Weight changes in mice receiving i.t. inoculum of RP73-laden agar beads ($\sim 3.5 \times 10^6$ CFU/mouse) and relative total leukocytes (**e**), PMN, and monocyte/MΦ (**f**) number in BAL at the indicated time point following challenge with agar-enmeshed RP73. (**g**) Histopathology of lung microsections during chronic RP73 infection. Photomicrographs are representative from 4–10 mice/data point. (**h**) Levels of LTB_4 and the biogenic precursor of RvD1 17-HDoHE in lung homogenates at early and late phase of chronic RP73 infection. Amount of each lipid mediator was determined by taking into account the total homogenate volume. Results are mean ± s.e.m. from 3 independent experiments with 15 mice. The lower panel shows a representative multiple reaction monitoring MS/MS spectrum of 17-HDoHE identified by the LC-MS/MS diagnostic ions indicated in **Table 2**. (i) Levels of select cytokines and chemokines in lung homogenates during RP73 chronic infection. $^*P < 0.05$; $^{**}P = 0.005$, $^{***}P < 0.001$ vs. uninfected mice. Results are mean ± s.e.m. from 2 (panels A-C) or 3 (**d**–**h**) independent experiments with 4 (0, 3, 5 DPI) or 10 mice (1, 7, 14, 21 DPI)/data point. Results in panel I are mean ± s.e.m. from three independent experiments with three (0 DPI) and five (5 and 21 DPI) mice/group.

limit for LC-MS/MS, whereas their precursors accumulated in late phases of RP73 infection: i.e., 15-HETE for LXA_4, 17-HDoHE for RvD1 and 14-HDoHE for Mar-1. These findings indicate a timely-regulated activation of distinct biosynthetic pathways in select phases of *P. aeruginosa* infection and may also suggest a defect in SPM production in chronic lung infection.

Levels of the pro-inflammatory proteins interleukin-1β (IL-1β), CXCL1/KC (the mouse IL-8), and CCL5/RANTES were also significantly higher at 21 DPI compared to

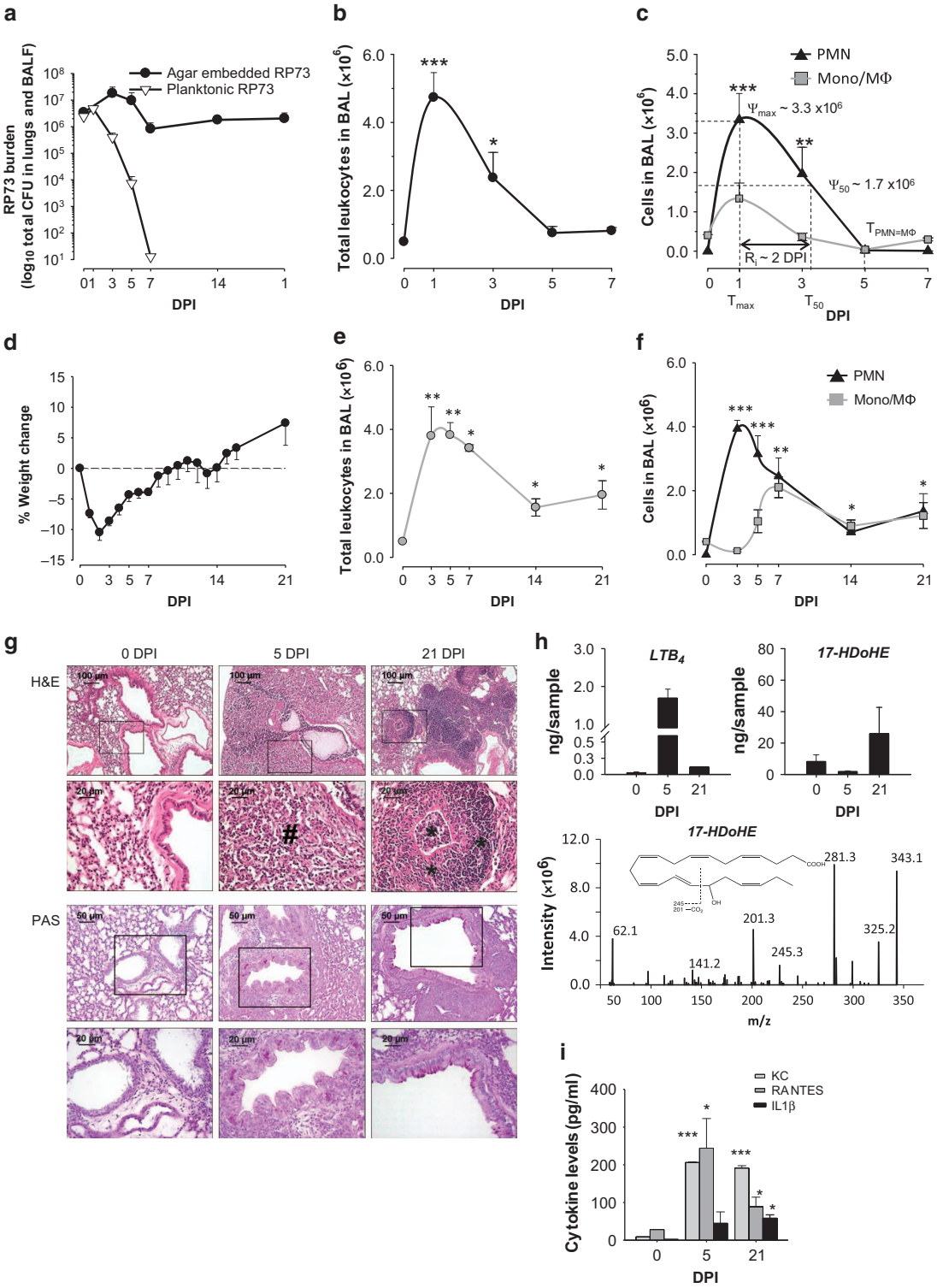

Table 1 Chronic *P. aeruginosa* infection-triggered lipidometabolomics

Mediator/ precursor			DPI		
			0	5	21
	Q1	Q3	Mean ± s.e.m.	Mean ± s.e.m.	Mean ± s.e.m.
PGE_2	351	271	3.70 ± 0.14	6.51 ± 2.60	21.17 ± 0.66
6-keto-PGF_{1a}	369	163	45.99 ± 20.35	43.82 ± 32.07	190.54 ± 109.97
$PGF_{2\alpha}$	353	193	1.62 ± 0.42	2.40 ± 0.90	2.68 ± 0.67
TXB_2	369	169	9.84 ± 4.53	6.72 ± 5.93	48.83 ± 51.01
LTB_4	335	195	0.03 ± 0.01	1.69 ± 0.24	0.12 ± 0.00
LTC_4	624	272	*	*	*
LTD_4	495	177	0.037 ± 0.002	35.071 ± 2.759	*
5-HETE	319	115	0.65 ± 0.04	5.56 ± 0.47	0.91 ± 0.17
15-HETE	319	219	4.61 ± 0.29	3.36 ± 1.20	14.23 ± 10.39
18-HEPE	317	259	*	0.03 ± 0.01	0.10 ± 0.02
7-HDoHE	343	141	0.08 ± 0.02	0.58 ± 0.11	0.06 ± 0.01
14-HDoHE	343	205	8.37 ± 0.10	8.76 ± 0.83	71.37 ± 15.09
17-HDoHE	343	245	8.33 ± 4.15	1.89 ± 0.45	25.91 ± 16.83
7,17-diHDoHE	359	119	*	0.13 ± 0.05	0.16 ± 0.06
10,17-diHDoHE	359	153	0.04 0.02	0.02 ± 0.00	0.47 ± 0.29

Abbreviations: DPI, days post infection; HDoHE, hydroxy-docosahexaenoic acid; HEPE, hydroxyeicosapentaenoic acid; HETE, hydroxyeicosatetraenoic acid; PG, prostaglandin; TX thromboxane.
Select lipid mediators and precursors/markers of biosynthetic pathways in lung homogenates from mice undergoing long term infection with RP73. Results are expressed as mean ± s.e.m. of ng/sample from two (0 DPI) or five (5 and 21 DPI) mice. *, below limits

non-infected mice (**Figure 1i**), providing a further biochemical evidence for a non resolving inflammatory state associated with a long term *P. aeruginosa* infection.

RvD1 treatment regulates leukocyte infiltration and lowers bacteria burden during *P. aeruginosa* lung infection

In this setting, we tested actions of RvD1 on *P. aeruginosa* clearance and inflammation. In mice challenged with planktonic RP73, a single oral administration of RvD1 (100 ng/mouse) by intragastric gavage (chosen as a delivery mode given the lower invasiveness compared to intravenous or intratracheal injection) significantly reduced lung bacterial titer by ~50% ($6.03 \pm 1.9 \times 10^6$ (RvD1) vs. $12.90 \pm 1.3 \times 10^6$ CFU (Veh)) and BAL accumulation of total leukocytes ($2.71 \pm 0.47 \times 10^6$ (RvD1) vs. $4.73 \pm 0.73 \times 10^6$ cells (Veh)), and PMN ($1.70 \pm 0.39 \times 10^6$ (RvD1) vs. $3.34 \pm 0.66 \times 10^6$ PMN (Veh)) at 1 DPI (**Figures 2a and b**). In contrast, oral gavage of RvE1 (100 ng/mouse), which also carries potent bioactions in airway tissues,[15] did not reduce infection ($11.25 \pm 1.9 \times 10^6$ CFU) and inflammatory cell accumulation in BAL (total leukocytes: $4.43 \pm 0.62 \times 10^6$; PMN: $3.52 \pm 0.70 \times 10^6$) indicating selective RvD1 bioactions against *P. aeruginosa* infection. When RvD1 was given to mice infected with agar-embedded RP73 starting from 3 h post bacterial challenge for 4 consecutive days (100 ng/mouse/day), it significantly reduced mortality (**Figure 2c**) and cachexia (**Figure 2d**) in the first days following infection. This was associated to a significant reduction in IL-1β and total protein levels in BAL as well as in Evan's blue leakage in lungs (**Figure 2e**) in RvD1-treated mice, which suggest that early protection conferred by RvD1 can be secondary to diminishing vascular and epithelial permeability following bacterial challenge.

P. aeruginosa burden (**Figure 2f**), total leukocytes, and PMN (**Figure 2g**) were also significantly lowered by RvD1 at 5 DPI, whereas monocyte/MΦ and lymphocyte numbers were unchanged, indicating enhancement of bacterial containment and counter-regulatory actions on leukocyte trafficking. Furthermore, while vehicle-treated animals were profoundly lethargic and poorly responsive to stimuli, mice receiving RvD1 showed a normal behavior with no apparent signs of pain (e.g., self-isolation, reduced motility, and tremor) (**Supplementary Movie S1 online**).

Thus, RvD1 limits the severity of *P. aeruginosa* pneumonia when administered early after infection.

RvD1 promotes the resolution of inflammation in infected airways and protects from tissues damage

We next asked whether RvD1 was also effective when given at the peak of infection. To this end, mice were infected with agar-embedded RP73 and left untreated for 5 days, when they were randomized to receive RvD1 (100 ng/mouse) or vehicle every 48 h up to 21 DPI. Treatment with RvD1 led to a significant reduction in lung RP73 titer both at 14 ($1.09 \pm 0.11 \times 10^6$ (RvD1) vs. $1.81 \pm 0.23 \times 10^6$ CFU (Veh)) and 21 DPI ($2.99 \pm 2.76 \times 10^5$ CFU (RvD1) vs. $2.03 \pm 0.13 \times 10^6$ CFU (Veh)) (**Figure 3a**). Remarkably, PMN and lymphocyte numbers in BAL decreased from 5 to 14 or 21 DPI in veh-treated mice, indicating the existence of endogenous resolution programs in response to *Pseudomonas* infection. RvD1 treatment further activated this program, reducing both PMN and lymphocyte numbers in BAL at 14 and 21 DPI (**Figures 3b and c**), giving in a marked change in resolution indices. In particular, RvD1 reduced PMN T_{50} from ~12 to ~10 DPI and lymphocyte T_{50} from ~13 to ~11 DPI, giving a left-shift in the R_i of ~2 days (**Table 2**).

These and previous findings showing adjunctive effects of SPM and antibiotics[18,21,23] prompted us to test RvD1 in combination with ciprofloxacin and levofloxacin, leading drugs for *P. aeruginosa* infections. To this end, we first determined susceptibility of RP73 to both antimicrobials. As shown (**Table 3**) ciprofloxacin was more potent than levofloxacin in inhibiting *in vitro* growth of RP73, although MIC values of both antimicrobials on RP73 were higher than those required for inhibiting the PA01 reference strain, confirming that clinical isolates of *P. aeruginosa* are prone to acquire resistance.[39] Consistent with this, ciprofloxacin at 200 and 400 μg/day gave a dose-dependent reduction in RP73 titer

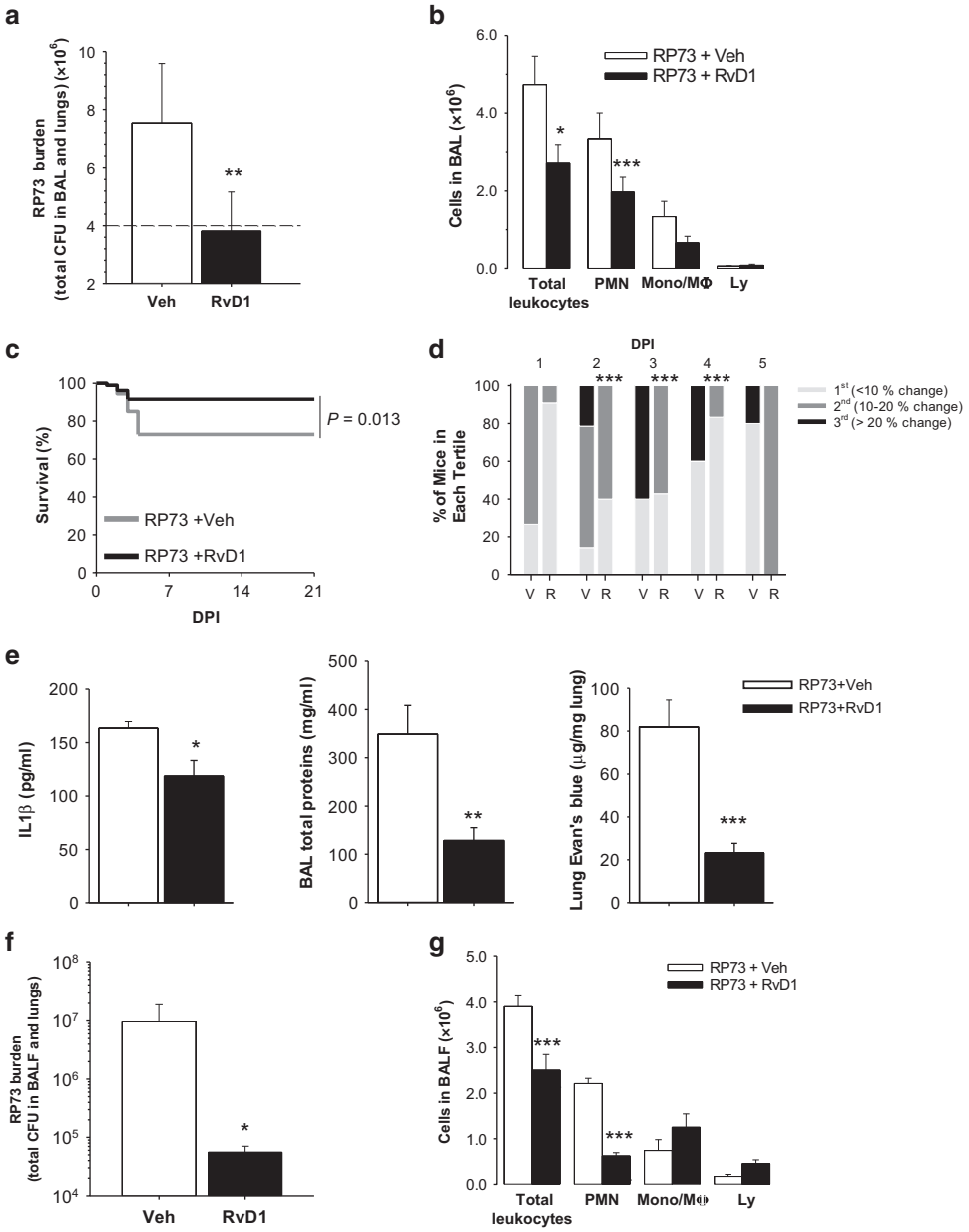

Figure 2 RvD1 reduces RP73 load and leukocyte infiltration in acute and chronic lung infection. (**a**, **b**) Total numbers of live bacteria and inflammatory cells in mice receiving gavage (200 μL of saline) plus vehicle (0.5%$_{vol/vol}$ EtOH/mouse) or RvD1 (100 ng/mouse) 3 h post intratracheal inoculum with planktonic RP73. BAL and lungs were collected at 1 DPI. $^{*}P = 0.021$; $^{**}P = 0.041$; $^{***}P = 0.027$. Results are mean ± s.e.m. from 2 independent experiments with 11 (vehicle-treated group) and 12 (RvD1-treated group) mice. (**c**–**e**) Differences in survival, weight loss, and indexes of lung permeability. Mice receiving intratracheal inoculation of RP73-charged agar beads were treated with vehicle (0.05%$_{vol/vol}$ EtOH/mouse, per os) or RvD1 (100 ng/mouse/day per os) via gavage 24 h following inoculum. BAL levels of IL-1β, total proteins, and Evan's Blue amounts were determined at 5 DPI. $^{*}P = 0.018$; $^{**}P = 0.002$; $^{***}P < 0.001$. Results are pooled from 2 independent experiments with 12 mice/group. V, vehicle-treated mice; R, RvD1-treated mice. (**f**, **g**) Total CFU and leukocytes in vehicle- or RvD1-treated mice infected with agar-embedded RP73 determined 5 days post agar bead inoculum. $^{*}P = 0.023$; $^{***}P < 0.001$. Results are mean ± s.e.m. from 2 experiments with 12 mice/group.

in vivo without leading to complete eradication (**Figure 3d**). Remarkably, administration of RvD1 (as low as 100 ng/day) was as potent as ciprofloxacin (given at 200 μg/day daily dose) in reducing *P. aeruginosa* burden (**Figure 3e**) and inflammatory cell numbers in BAL (**Figure 3f**). Of interest, the combination of the two compounds further diminished bacterial load in the airways, demonstrating that RvD1 provides additional benefits to the sole antibiotic therapy (**Figure 3e**), while such additive effect was not evident on BAL leukocyte numbers.

To determine mechanisms underlying RvD1 actions, we measured phagocytosis of *P. aeruginosa in vitro* and *in vivo*, which is a defining bioaction of SPM pivotal for microbial killing.[7,14] *In vitro* treatment of murine RAW 264.7 MΦs with

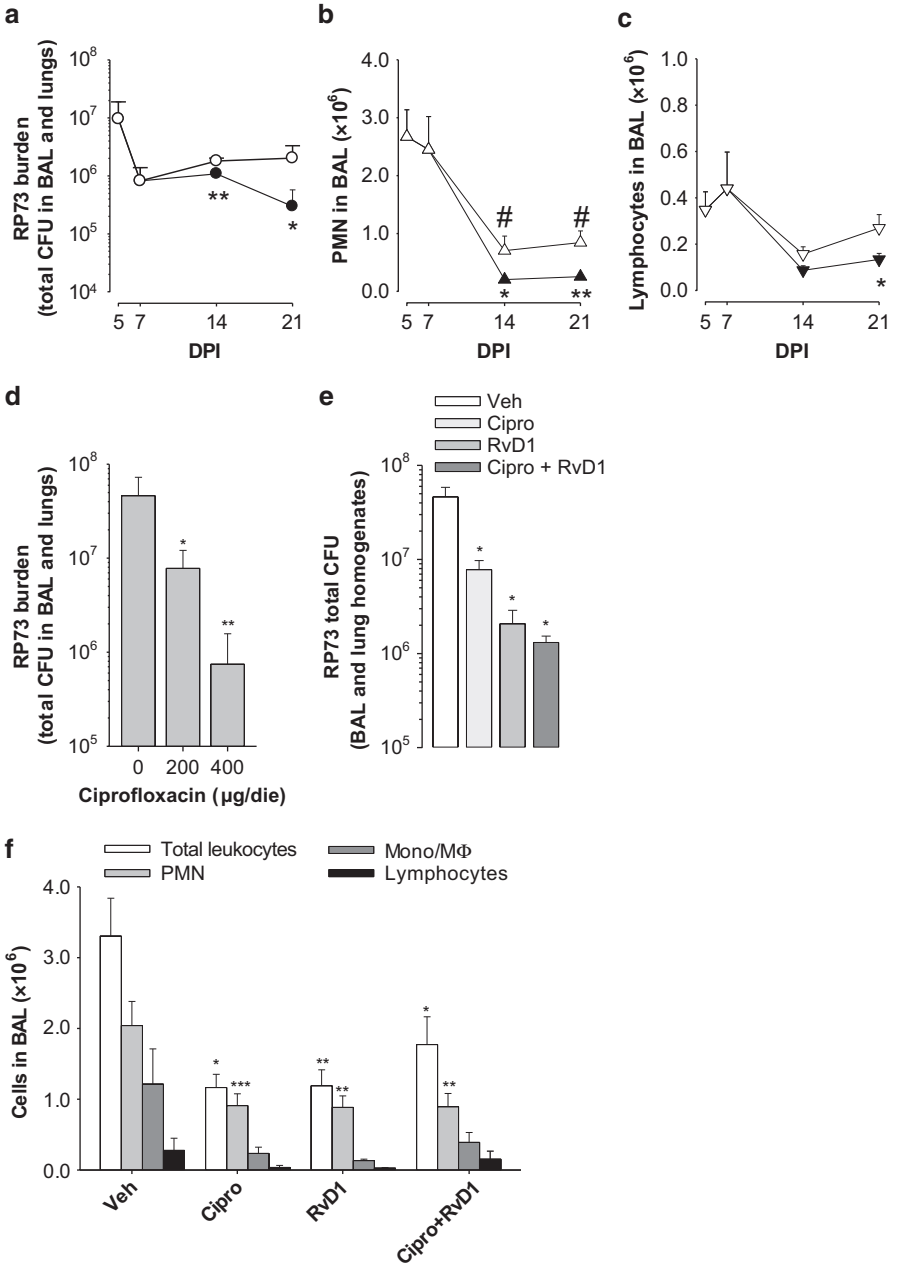

Figure 3 RvD1 enhances bacterial clearance and resolution in chronic *P. aeruginosa* infection synergizing with ciprofloxacin. (**a**-**c**) Bacterial load and inflammatory cell infiltrates in mice infected with RP73 agar beads ($\sim 3.5 \times 10^6$ CFU/mouse) that received oral gavage with vehicle or RvD1 (100 ng/mouse) every 48 h starting from day 5 post inoculum. Numbers of live RP73 CFU, PMN, and lymphocytes were determined at 14 and 21 DPI. Quantitative resolution indices for PMN and lymphocyte removal are indicated in panels B and C. Results are mean ± s.e.m. from 2 separate experiments with 10 mice/group. $^{\#}P<0.05$ vs. 5 DPI; $^{*}P<0.05$; $^{**}P<0.01$; vs. veh-treated mice. (**d**) Effect of ciprofloxacin on chronic *P. aeruginosa* lung infection. Mice infected via i.t. inoculum of agar-embedded RP73 treated with vehicle or ciprofloxacin (200, 400 μg/day, i.p.). RP73 titer in BAL and lung homogenates was determined 5 days post infection. Results are mean ± s.e.m. from 7-10 mice/group. (**e**, **f**) Effect of combined RvD1 and ciprofloxacin treatment on RP73 infection, inflammation, and bacterial clearance. Bacterial load in BAL and lung homogenates and BAL cell counts were determined 5 days following inoculum of RP73 in agar beads in mice treated daily with vehicle (0.5% EtOH) or RvD1 (100 ng, os) alone or in combination with ciprofloxacin (200 μg, i.p.). Results are mean ± s.e.m. from 2 separate experiments with 10–15 mice/group. $^{*}P<0.05$; $^{**}P<0.01$; $^{***}P<0.001$ vs. veh-treated mice.

RvD1 (0.01–100 nM) prior infection with fluorescent RP73 cells resulted in a dose-dependent enhancement of phagocytosis (**Figure 4a**). To measure *in vivo* phagocytosis, BAL leukocytes collected 5 days following infection with agar-embedded RP73 were permeabilized and incubated with an anti-*P. aeruginosa* antibody in order to detect ingested bacteria with flow cytometry. As shown, RvD1 gave a significant enhancement in phagocytosis of *P. aeruginosa* by BAL PMN and MΦs 5 days following infection, which was further potentiated by ciprofloxacin co-administration as indicated by (**Figure 4b**).

Table 2 Resolution indices for chronic *P. aeruginosa* infection

	PMN		Lymphocytes	
	Vehicle	RvD1	Vehicle	RvD1
Ψ_{max}	$3.14 \pm 0.57 \times 10^6$	NA	$0.44 \pm 0.16 \times 10^6$	NA
Ψ_{50}	1.57×10^6	NA	0.22×10^6	NA
T_{max}	5 DPI	5 DPI	7 DPI	7 DPI
T_{50}	12 DPI	10 DPI	13 DPI	11 DPI
R_i (T_{50}–T_{max})	7 DPI	5 DPI	6 DPI	4 DPI

Abbreviations: DPI, days post infection; PMN, polymorphonuclear neutrophil. Resolution indices were calculated from BAL PMN and lymphocyte numbers in mice challenged with agar-embedded RP73 and treated with RvD1 (100 ng every 2 days) or vehicle from day 5 after infection up to 21 DPI.

Table 3 Susceptibility of *P. aeruginosa* strains to ciprofloxacin and levofloxacin

***In vitro* MIC (μg/ml)**	Strain	
	PA01	RP73
Ciprofloxacin	0.0556 ± 0.006	0.875 ± 0.072
Levofloxacin	0.3150 ± 0.046	7.000 ± 1.500

In vitro MIC determined on TSA plates using the ε-test are reported as mean ± s.e.m. from four independent experiments.

Also, since Abdulnour and colleagues recently showed that 17*R*-RvD1 increases the antimicrobial protein lipocalin 2 during *E. coli* acute pneumonia,[21] we measured this endogenous peptide in RvD1 treated mice. As shown, RvD1 significantly increased BAL levels of lipocalin 2 at 5 DPI (**Figure 4c**), demonstrating the ability to boost innate host defenses.

Since RvD1 treatment gave a significant reduction in PMN and lymphocyte accumulation in BAL of chronically infected mice, we examined if RvD1 stimulated their active removal *in vivo*. To this end, BAL MΦs collected 14 and 21 DPI from veh- or RvD1-treated mice were permeabilized and counterstained with anti-Ly6G and CD3ε antibodies to detect ingested neutrophils and lymphocytes with flow cytometry (see **Supplementary Method**). As shown, RvD1 significantly increased phagocytosis of PMN and lymphocytes at 14 and 21 DPI, as indicated by the enhanced Ly6G- or CD3ε-intracellular staining of MΦs (**Figure 4d**). Hence, these results highlight the existence of endogenous resolution mechanisms that are potentiated by RvD1.

To better define pro-resolution activity of RvD1, we assessed histological signs of lung inflammation and damage. Histopathological analyses revealed that RvD1 significantly decreased intraluminal granulocyte and peribronchial lymphocyte infiltrates, as well as parenchymal involvement and MuSC metaplasia (**Figure 5a**). Moreover, it significantly diminished bronchiolar cell hyperplasia, as indicated by a reduction in epithelial thickness (**Figure 5b**), an established histological marker of lung pathology and respiratory impairment.

Thus, RvD1 lowered *P. aeruginosa*-triggered lung inflammation, enhanced bacterial and leukocyte clearance and protected lung tissue from non resolving *P.aeruginosa* infection.

RvD1 regulates select genes and miRNAs in lung MΦs and carries direct actions on human phagocytes

In order to define molecular mechanisms of RvD1 bioactions, on the basis of early data showing that it regulates select genes and miRNAs in MΦs,[30,31,33] we investigated RvD1-induced changes in expression levels of genes involved in innate and adaptive immune responses in lung MΦs *in vivo*. To this end, lung MΦs expressing the $CD45^+/CD11b^+/CD11c^+/F4/80^+$ phenotype (**Figure 6a**) were sorted from mice bearing chronic infection and treated with RvD1 or vehicle. Differential analyses carried out on a panel of 84 genes, using quantitative PCR and bioinformatic analyses, showed that RvD1 significantly downregulated several genes linked to pathogen recognition and downstream pro-inflammatory signaling pathways. In particular, RvD1 reduced transcripts of TLR2, 4 and 6, Myeloid differentiation primary response gene 88 (MyD88), and TIR Domain-Containing Adapter Protein Inducing IFN-Beta (TRIF) by >1.5 fold (**Figures 6b** and **c**). Genes activated by MyD88 and TRIF, such as Myxovirus resistance 1 (Mx1), C reactive protein (CRP), myeloperoxidase (MPO), CCR4, CCL5/RANTES, and CXCL10/IP10 (**Figures 6c** and **7a**) were also significantly reduced by RvD1. Of note, although tumor necrosis factor-α (TNF-α), TNF receptor-associated factor 6 (TRAF6), IL-1β, and IL-17 mRNAs showed a reduction in MΦs from RvD1-treated mice, this did not attain significance (TNF-α $= -1.67$ fold change, $P = 0.057$; TRAF6 $= -1.68$, $P = 0.058$; IL-1β $= -2.49$, $P = 0.24$; IL-17 $= -1.28$, $P = 0.82$).

Since RvD1 regulates miRNAs[30,31] that are pivots in dampening TLR signaling pathways in MΦs during inflammation,[40] we searched the Ingenuity Pathway Analysis (IPA) database for miR with binding sequences to the 3′ untranslated region of RvD1-downregulated genes and assessed their level in MΦs sorted from murine lungs. IPA indicated that miR-10, -146b, and -155 can decrease MyD88 expression by binding its 3′ untranslated region mRNA, whereas the TLR2 mRNA is a direct target of miR-21 and miR-21 and -155 regulate CXCL10, TNF-α, and IL-17 (**Figure 7a**). As shown in **Figure 7b**, RvD1 significantly increased miR-21 and miR-155 levels, but not miR-10 and -146b, suggesting that selected microRNAs are part of the molecular mechanisms of RvD1 actions on MΦs during chronic *P. aeruginosa* infection.

To further validate these results, we measured cytokines, chemokines, and growth factors involved in lung inflammation in lung fluids from RvD1- or vehicle-treated infected mice. Consistent with mRNA and miRNA analyses, RvD1 significantly reduced protein levels of CCL5, CXCL10/IP10, CXCL1/KC, IL-1β, IL-17, and vascular endothelial growth factor (VEGF), all downstream effectors of the TLR-MyD88/TRIF pathway (**Figure 7c**).

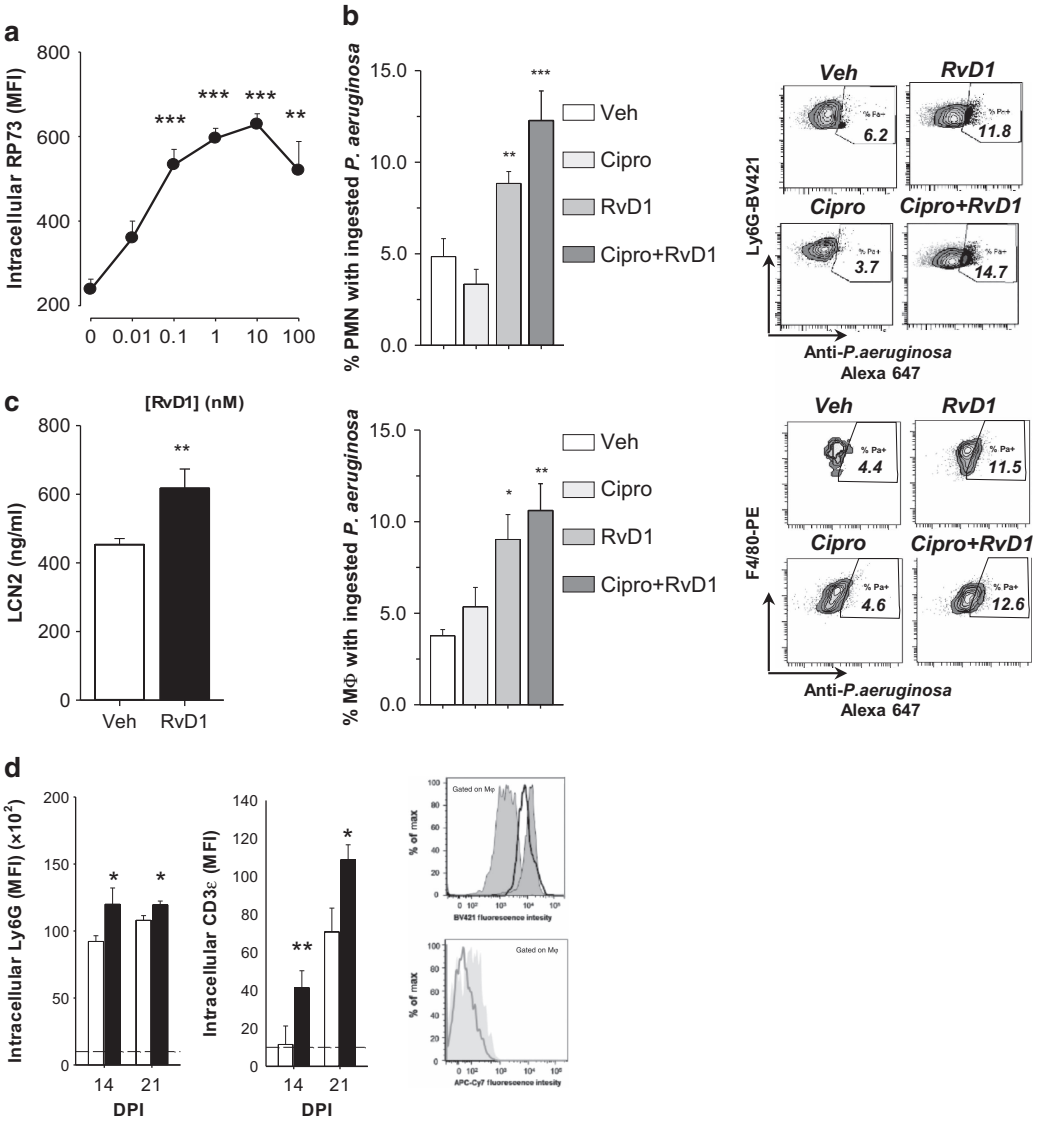

Figure 4 Resolvin D1 enhances phagocytosis of *P. aeruginosa* and leukocytes by MΦs. (**a**) Concentration-dependent increase in phagocytosis of RP73 cells induced by RvD1 in murine RAW 264.7 MΦs. FITC-labeled RP73 (1×10^6, 37 °C, 90 min) was added to cells (2×10^5) treated with RvD1 or vehicle (15 min, 37 °C). Phagocytosis was assessed by measuring intracellular FITC Mean Fluoresce Intensity (MFI). Results are mean ± s.e.m. from three experiments with quadruplicates. $^{**}P<0.01$; $^{***}P<0.001$ vs. vehicle-treated cells. (**b**) *In vivo* phagocytosis in mice infected with RP73-laden agar beads was determined with flow cytometry upon permeabilization and staining of BAL neutrophils ($CD11b^+/Ly6G^+$ leukocytes) and MΦ ($CD11b^+/F4/80^+$ leukocytes) with an anti-*P. aeruginosa* antibody (1 μg/5×10^5 cells) followed by an Alexa 647-tagged secondary antibody (10 μg/ml). BAL were collected 5 DPI. Right panel shows a representative flow cytometry dot plots. Results are mean ± s.e.m. from 8–15 mice/group. $^{*}P<0.05$; $^{**}P<0.01$; $^{***}P<0.001$ vs. vehicle-treated mice. (**c**) Lipocalin 2 levels in BAL collected 5 DPI from vehicle- or RvD1-treated mice. Results are mean ± s.e.m. from 8 to 9 mice/group. $^{*}P<0.05$; $^{**}P<0.01$; $^{***}P<0.001$ vs. vehicle-treated mice. (**d**) RvD1 stimulates phagocytosis of PMN and lymphocytes by lung MΦs *in vivo*. Lung MΦs from infected mice treated with vehicle or RvD1 (100 ng/mouse) every 48 h from 5 DPI were collected at the indicated time points, labeled (15 min, 4 °C) with PE-anti-F4/80 (0.2 μg/5×10^5 cells), permeabilized, and counter-stained (30 min, 4 °C) with BV421-anti-Ly6G (for PMN) or APC-Cy7-anti-CD3ε (for T lymphocytes) antibodies. Intracellular fluorescence of $F4/80^+$-MΦ associated with ingested PMN or lymphocytes was determined by flow cytometry. $^{*}P<0.05$; $^{**}P<0.01$. Results are mean ± s.e.m. from 5 to 8 mice/data point. Representative flow cytometry histograms of intracellular staining of MΦs from RvD1- (filled histograms) vs. vehicle- (open histograms) treated mice are shown on right. Gray histograms are negative controls from F4/80 and Ly6G-or CD3ε-stained MΦs without permeabilization.

Together, these results provide molecular mechanisms of RvD1 action that lower inflammatory signaling in lung MΦs in response to *P. aeruginosa*.

For translational purposes, we assessed bioactions of RvD1 in human systems. As shown, RvD1 significantly enhanced phagocytosis of fluorescent RP73 by peripheral blood human PMN (**Figure 8a**) and monocyte-derived MΦs (**Figure 8b**), recapitulating *in vivo* actions. In contrast, RvD1 diminished TNF-α-induced activation of pulmonary artery endothelial cells (indicated by CD62E/E-selectin and CD54/ICAM1 surface expression) and endothelial-PMN interactions (assessed by monitoring changes in electric impedance to

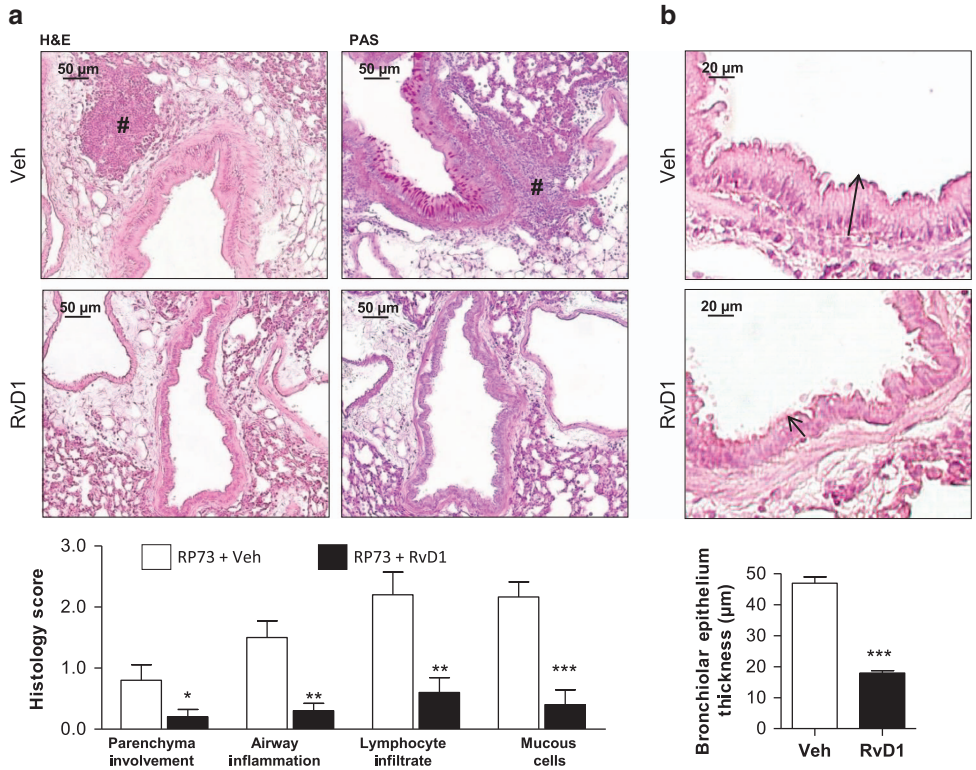

Figure 5 Resolvin D1 is organ protective in chronic *P. aeruginosa* infection and enhances non phlogistic clearance of *P. aeruginosa* and inflammatory cells by macrophages. Histopathology and semiquantitative scores of (**a**) inflammation and mucous metaplasia and (**b**) bronchiolar epithelial hyperplasia of lung sections collected at 21 DPI from infected mice receiving vehicle or RvD1 (100 ng/mouse) every 48 h from day 5 following inoculum. Photomicrographs are representative from 5 mice/group. Semiquantitative scores are mean ± s.e.m. from two experiments with five mice/group. $^{*}P<0.05$; $^{**}P<0.01$; $^{***}P<0.001$.

quantify neutrophil diapedesis across endothelial cells). In addition, RvD1 blunted the decrease in endothelia cell layer impedance induced by IL-1β, a measure of loss in barrier function and increase of vascular permeability in response to inflammatory stimuli (**Supplementary Figure S1**).

Collectively, these results indicate that RvD1 carries multi-pronged actions on human cells that boost host-defensive phagocytic activity against *P. aeruginosa* infection while limiting leukocyte recruitment and vascular responses.

DISCUSSION

P. aeruginosa is a global health threat since it sustains infections often difficult to eradicate, triggering non resolving inflammatory processes that lead to disability and death.[1] Therefore, there is an unmet need for new strategies to combat *P. aeruginosa* infections and inflammation. Here, we provide preclinical evidence that RvD1 is protective in acute and chronic lung infection caused by a clinical strain of *P. aeruginosa*. When given therapeutically to *P. aeruginosa*-infected mice, RvD1 markedly reduced bacterial load, dampened leukocyte accumulation, enhanced bacterial clearance potentiating the efficacy of ciprofloxacin, and activated removal of infiltrated leukocytes by MΦs. RvD1 protected lung tissue, reducing parenchymal inflammation, mucus metaplasia, and bronchiolar hyperplasia. Mechanistically, we demonstrated that RvD1 regulated select genes and miRNAs involved in pathogen recognition and inflammatory signaling in MΦs *in vivo*, blunted PMN-EC interactions, and enhanced *P. aeruginosa* phagocytosis by human leukocytes.

The RP73 strain of *P. aeruginosa* used in this study is a clinical isolate derived from the airways of a cystic fibrosis patient at a late stage of infection. It is endowed with virulence factors, phenotypic traits, and adaptation capacity that confer advantages for establishing long-term infections and resistance to antibiotics.[5,41] In order to create a stable colonization of mice lungs, *P. aeruginosa* must be immobilized in polysaccharide-rich matrices to mimic the growth in the mucus of infected patients[37] and reproduce histological hallmarks of chronic human infections.[38] Congruently, challenge with agar-embedded RP73 triggered a long lasting bacterial infection in mice and a sustained inflammatory reaction characterized by leukocyte recruitment, airway tissue damage, and enhanced release of pro-inflammatory cytokines (**Figure 1**). Moreover, we observed changes in the lipid mediator profile of lung tissues chronically infected with RP73. For instance, 5-LO-derived LTB_4, a primary leukocyte-derived chemoattractant, and LTD_4, which mediates vascular permeability and bronchoconstriction,[42] as well as 5-HETE, increased rapidly after infection. This is consistent with the initial recruitment in the infected lung of PMN, which express high levels of

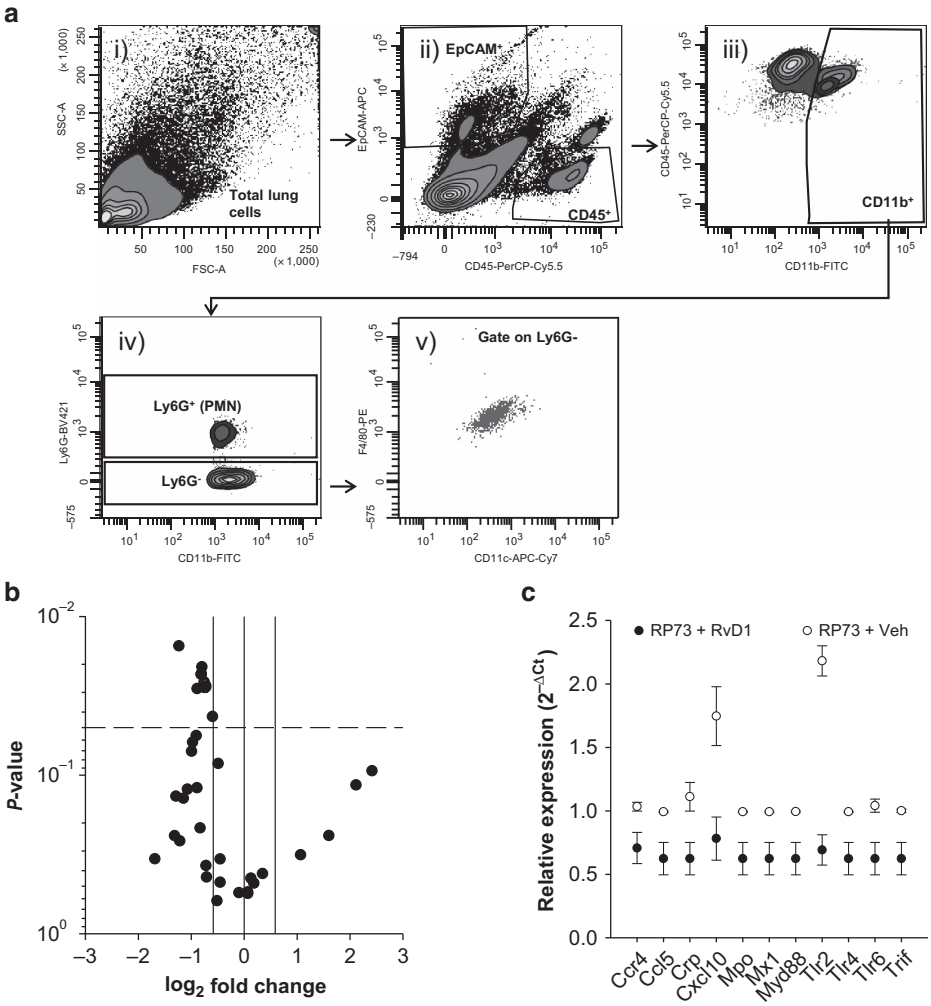

Figure 6 Select genes regulated by RvD1 in lung MΦs during chronic *P. aeruginosa* infection. (**a**) Representative FACS dot plots showing gating strategies for the isolation of $CD11b^+/CD11c^+/F4/80^+$ lung MΦs. (**b**) The Volcano plot displays significant changes in gene expression determined 5 days post infection with agar-embedded RP73 in lung MΦs sorted from RvD1- or vehicle-treated mice. Real time PCR analyses were carried out from 4 mice/group using the $2^{-\Delta Ct}$ method with GAPDH (NM_008084), GUSB (NM_010368), actin B (NM_007393), beta-2 microglobulin (NM_009735) and HSP90AB1 (NM_008302) as housekeeping reference genes. Fold changes were calculated as ratios of $2^{-\Delta Ct}$ values between MΦs from RvD1-and vehicle-treated mice. The dashed line represents the $P = 0.05$ value used as a cut-off for selecting genes significantly regulated by RvD1. (**c**) Relative expression of genes with a significant ($P < 0.05$) fold change induced by RvD1. Results are mean ± s.e.m. from four mice/group.

metabolically active 5-LO. On the contrary, PGE_2, $PGF_{2\alpha}$, 6-keto-$PGF_{1\alpha}$ (a PGI_2 further breakdown product) and thromboxane (TX) B_2 (a TXA_2 biomarker), involved in oedema formation, vascular, and regulation of endothelial-leukocyte interactions[42] reached a maximum 21 DPI, likely as a reflection of changes in cellularity and activation of parenchymal cells. 14-HDoHE and 17-HDoHE, precursors of D-series resolvins and maresins, also increased during infection. Of note, although RvD1 has been identified in several mouse tissues[13,18,27] and, more recently, in human plasma from patients with pulmonary tuberculosis,[43] and arthritic synovial fluids,[16] it was below the LC-MS/MS detection limit in infected mice, likely reflecting the lack of proper transcellular exchanges required for RvD1 biosynthesis.[28] Lack of biosynthesis of SPM investigated here could also represent a distinct defect of chronic *P. aeruginosa* infection. Along this line, recent studies demonstrate that a secreted *P. aeruginosa* protein abundantly found in sputum of patients with cystic fibrosis disrupts the biosynthesis of 15-epi-LXA4.[44] Overall, our data are consistent with the switch, observed in humans[45] as well as in preclinical models,[13,45,46] in the biosynthesis of AA-derived PG and LT, which are predominant in the early phase of an inflammatory response, to SPM, which accumulate at a later time.

SPM limit the severity of infection caused by several bacterial species and promote timely resolution. For instance, RvD2 reduces mortality and bacterial dissemination after cecal ligation puncture-induced sepsis,[17] 17*R*-RvD1 stimulates resolution of *E. coli* acute pneumonia,[21] and RvD1 and D5 both enhance clearance of *E. coli* peritonitis and *S. aureus* skin infection.[18] In these early studies, RvD1 and 17*R*-RvD1 proved to potentiate *in vivo* efficacy of antibiotics in eradicating infections and lowering leukocyte numbers in exudates.[18,21] Here, effects of RvD1 plus ciprofloxacin were additive on RP73

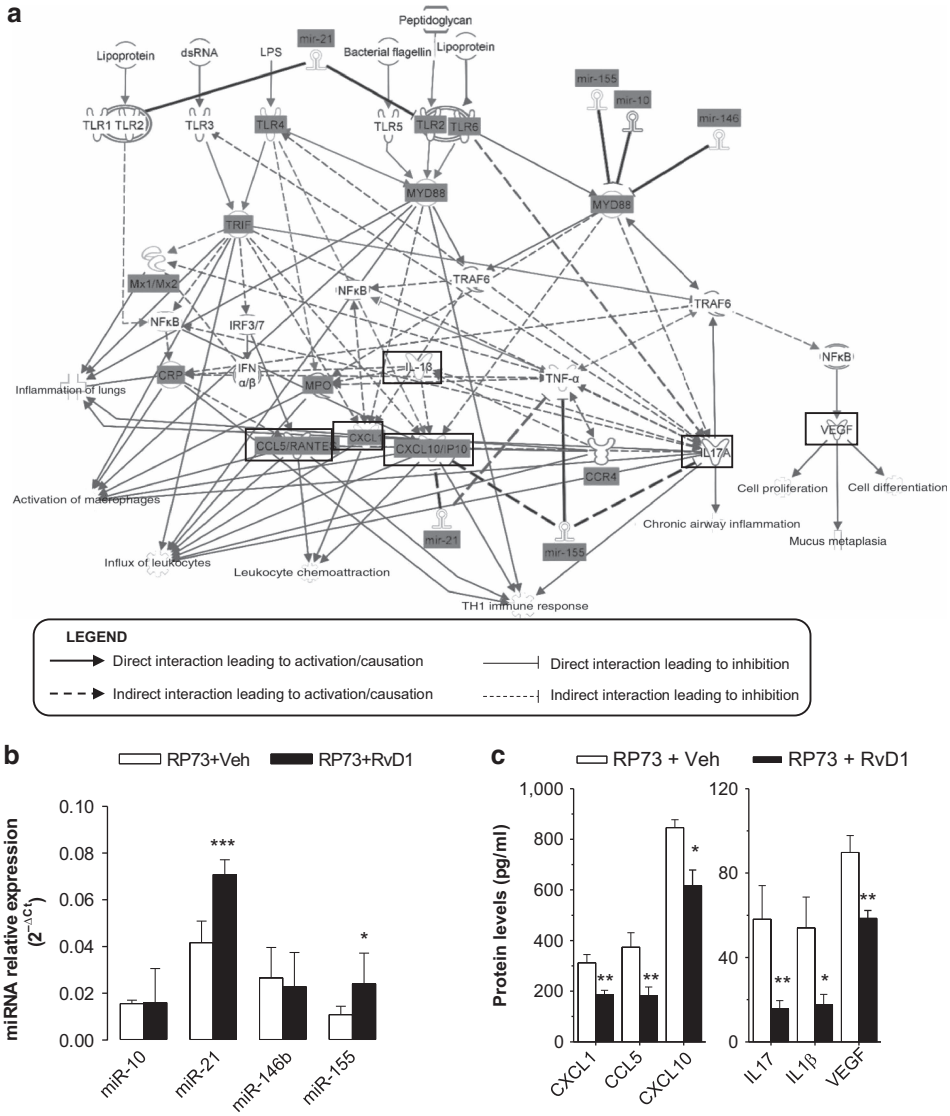

Figure 7 RvD1-regulated molecular pathway controlling inflammation and resolution signaling in MΦs during chronic *P. aeruginosa* infection. (**a**) The IPA map displays connections between RvD1-regulated genes and miRNAs and their functional roles in the regulation of MΦ responses to pathogens. The figure shows direct (solid lines) or indirect (dashed lines) connections between genes and miRNAs that lead to activation/causation or inhibition of indicated functions. Genes found significantly regulated by RvD1 using real time PCR analyses are indicated by filled labels. Genes encoding for proteins whose levels were determined are within boxes. (**b**) miRNAs regulated by RvD1 in sorted lung MΦs during RP73 infection, determined using real-time PCR. Results are mean ± s.e.m. from 4 mice/group. $^{*}P = 0.029$; $^{***}P < 0.001$ vs. MΦs from vehicle-treated infected mice. (**c**) Proteins encoded by RvD1-regulated genes, determined in lung homogenates 21 after infection with agar-embedded RP73 in mice treated with RvD1 or vehicle starting from day 5. Results are mean ± s.e.m. from 6 to 9 mice/group. $^{*}P < 0.05$; $^{**}P < 0.01$.

titer, but not on BAL leukocyte and PMN counts. This may depend on the greater complexity of chronic lung infection used in this study compared to the self-resolving systems used in previous reports, or by the fact that the RP73 strain used here is a multi-drug resistant isolate evolutionarily adapted to cause persistent, non resolving lung inflammation that are resistant to therapies.

Like other SPM, does not inhibit bacterial growth *per se*.[17,18] Thus, enhancement of phagocytosis represents a main cellular mechanism by which they enhance resolution of infection. Consistent with this, RvD1 significantly lowered RP73 burden in self-limited and chronic infection and stimulated its phagocytosis by mouse and human phagocytes. In addition, RvD1 increased levels of lipocalin, an iron chelating protein involved in microbial killing that is also regulated by 17R-RvD1, indicating that SPM can boost both cell-mediated and humoral defense mechanisms. Together with the evidence that RvD1 can be detected in human tissues[16,43] these results suggest that this SPM can be involved in the host response to bacterial colonization and that it has a therapeutic potential in human pharmacology, specially in clinical settings in which infections caused by multiple multi-drug resistant bacteria can occur, like in patients with cystic fibrosis.

MΦ from RvD1-treated mice showed enhanced capability to phagocytose PMN and lymphocytes (**Figure 4**), which is in keeping with the proresolution action of RvD1, since clearance

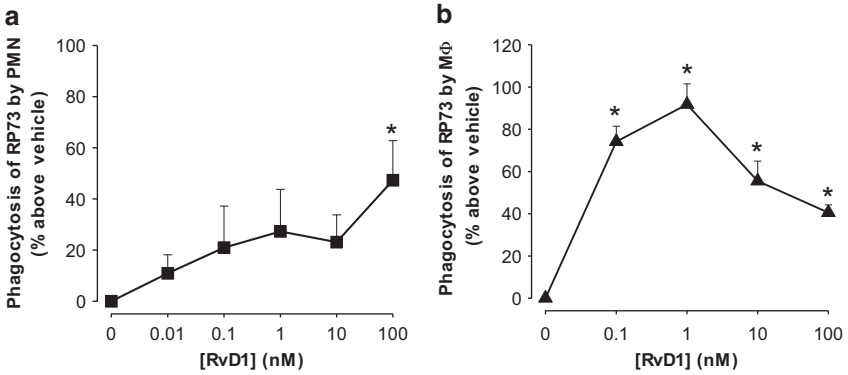

Figure 8 RvD1 enhances phagocytosis of *P. aeruginosa* by human leukocytes. Phagocytosis of FITC-labeled RP73 by human PMN in whole blood (**a**) or MΦs obtained from differentiated blood monocytes (**b**) treated (15 min, 37 °C) with the indicated concentrations of RvD1. Phagocytosis of RP73 was assessed by measuring fluorescence associated with PMN or MΦs using a flow cytometer or a plate reader, respectively. $^{*}P<0.05$; $^{**}P<0.01$; $^{***}P<0.001$ vs. vehicle. Results are mean ± s.e.m. from three experiments with determinations carried out as a quadruplicate. MFI, mean fluorescence intensity.

of infiltrated leukocytes by MΦs is the hallmark of the resolution phase of inflammation.[7] Histological analysis of the lung parenchyma confirmed that RvD1 potently reduced RP73-triggered inflammation by reducing leukocyte and lymphocyte tissue infiltration, mucous secretion and bronchiolar epithelium thickness (**Figure 5**). These results also emphasize the concept that SPM are crucial in preventing exacerbated leukocyte infiltration following infections, stimulating their removal, and ensuring tissue protection.

In vivo and in isolated cell systems RvD1 also stopped recruitment and infiltration of PMN, which have essential roles in innate defenses and clearance of *P. aeruginosa,* as demonstrated by preclinical and clinical studies. In experimental lung infections, neutrophil depletion in mice results in hypersusceptibility, with *P. aeruginosa* spreading, uncontrolled cytokine storm, and rapid death[47,48] and neutropenic patients have a higher risk of mortality due to *P. aeruginosa* bacteremia and septic shock.[49] In addition, recent clinical trial evaluating the safety of BIIL 284, a LTB4 receptor antagonist that blocks PMN recruitment in the lung, was prematurely terminated because of the increased incidence of pulmonary exacerbations in patients treated with the investigational drug, likely as a consequence of the impairment in neutrophil-mediated bacterial killing,[50] highlighting the narrow risk:benefit ratio of anti-inflammatories in the context of bacterial infections. Hence, dual actions of RvD1 on neutrophils (i.e., stop of their further infiltration and enhancement of phagocytic activity) reported here and in previous studies are remarkable.

We also investigated molecular mechanisms underlying RvD1 actions in chronic *P. aeruginosa* lung infection and demonstrated that RvD1 regulates specific genes and proteins in lung MΦs involved in leukocyte chemotaxis and infiltration (e.g., CCL5, CXCL10, and CXCL1), Th1 immune response and chronicity of airway inflammation (e.g., MyD88 and IL17), and cell activation (MyD88, TRIF, IL17) (**Figures 6 and 7**). RvD1 also reduced VEGF and IL17, which stimulate cell proliferation, airway remodeling, and metaplasia[51,52] (**Figures 6 and 7**). These results are in agreement with our findings that RvD1 limited excessive leukocyte infiltration, lung histopathology, and hyperplasia *in vivo*.

Of interest, many of the genes diminished by RvD1 in MΦ *in vivo* are controlled by miR-155 and miR-21, which were also upregulated by RvD1 during chronic *P. aeruginosa* infection. miR-155 and miR-21 have important roles in limiting the extent and the duration of inflammation. Indeed, by targeting TLRs and NF-κB, they prevent excessive or persistent stimulation of MΦs that can lead to unrestrained cell activation, overshooting cytokine and ROS release, and tissue destruction, which contribute to the pathogenesis of many diseases, including chronic pneumonia and cystic fibrosis.[40,53,54] RvD1 carries remarkable regulatory actions on MΦs via miRNAs and their target genes without suppressing their responsiveness to bacteria or other dangerous stimuli (e.g., microbial particles). During acute peritonitis induced by zymosan (a yeast cell wall component and a TLR2 ligand), and also in human MΦs, RvD1 regulates miR-21, miR-146b, miR-208a, and miR-219 and their target genes as an underlying mechanism to limit overzealous MΦ activation, reduce inflammation, and promote resolution.[30,31] For instance, the RvD1-regulated miR-146b targets IL-8, miR-208a controls IL-10, and miR-219 reduces 5-LO protein and biosynthesis LTB_4, which stimulates PMN recruitment.[30] In *E. coli*-infected MΦ, RvD1 dampens the expression of pro-inflammatory genes regulated via TLRs and NF-κB such as COX-2 together with stimulating bacterial uptake.[18] Along these lines, RvD2 also reduces TLR4 expression and signaling in human monocytes via miR-146a[55] and 17*R*-RvD1 dampens endotoxin- and *E. coli*-induced activation of human macrophages,[56] indicating that regulation of MΦ responses through miRNAs and TLRs is a common mechanism of action of SPM. Therefore, current findings on regulation of TLRs are congruent with the established concept that RvD1 (like other SPM) finely tunes MΦ responses to avoid perpetuation of inflammation without blunting their host defensive properties, a concept further

corroborated by the increase in *P. aeruginosa* clearance and phagocytosis observed in RvD1-treated mice and cells shown in the current study.

In conclusion, here we demonstrate that RvD1 is protective against persistent, non resolving inflammation caused by chronic lung infections with a clinical, multi resistant strain of *P. aeruginosa*. Our results unveil key cellular functions and molecular actions of RvD1 in host defense of airways mucosal tissues to pathogens, pointing to this SPM as to a prototype of new drugs to combat *P. aeruginosa* infections.

METHODS

Bacterial growth and mice infection. For acute infection with planktonic bacteria, the clinical strain of *P. aeruginosa* RP73[41] was grown in tryptic soy broth (TSB) to mid-log phase ($OD_{600\ nm} = 0.45 \pm 0.05$; $\sim 2 \times 10^8$ CFU/mL). Bacteria were washed, suspended in Dulbecco's phosphate buffered saline (DPBS) at $\sim 2 \times 10^7$ CFU/mL, and injected i.t. into mice. For chronic infection, 16 OD ($\sim$ 50 ml) of RP73 were included into 100-200 μm diameter tryptic soy agar (TSA) beads and used within 24 h (see **Supplementary Materials and Methods**). Male and female C57Bl6/N mice (8-12 week-old, 20-22 g) from Charles River (Calco, Italy) were husbanded in semi-barrier cages and fed Altromin (Rieper, Bolzano, Italy) chow pellet diet containing 7.5 g/kg ω-6 linoleic acid and 1.2 g/kg (as a mixture of 18:3, 18:4, 20:5, and 22:6) fatty acids. Upon anesthesia with 2,2,2,-tribromoethanol (500 mg/kg, i.p.), 30–50 μl of planktonic or agar embedded RP73 ($\sim 3.5 \times 10^6$ CFU/mouse) were injected i.t. into lungs with 22-g 0.9 × 25 mm i.v. catheters. RvD1 (100 ng/mouse) or equal amount of vehicle (0.5%$_{vol/vol}$ EtOH) were administered via intragastric gavage of 0.2 ml of saline. Mice were monitored daily for clinical signs of disease and those that lost $\geq$ 20% body weight or showed evidence of severe clinical disease were euthanized before the termination of the experiment. *In vitro* minimal inhibitory concentrations (MIC) of ciprofloxacin and levofloxacin on the RP73 and the PA01 reference strain (LMG 27638) were determined with ε-test strips (Liofilchem, Roseto degli Abruzzi, Italy).

BAL collection, lung homogenization, and analyses. BAL was collected after injection of 1 ml (× 3) sterile DPBS i.t. Total leukocytes were counted using Turk's solution and stained (15 min, 4 °C) with fluorochrome-tagged antibodies (0.2 μg/5 × 10^5 cells) (**Supplementary Methods and Methods**) before acquisition with a FACS Canto II flow cytometer (BD). Viable RP73 cells in BAL and aseptically dissociated lungs were determined upon serial dilutions (10^{-1} down to 10^{-6}), plating on TSA, and o.n. growth at 37 °C. Cytokines/chemokines/growth factors were measured with Luminex (Millipore, Vimodrone, Italy) multiplex arrays except for CXCL10, that was determined with a sandwich ELISA (Peptotech, London, UK). For LC-MS/MS-based lipidomics, lungs non subjected to BAL (which could markedly modify the lipid mediator profiles) were rapidly dissociated in ice, mixed with 2 × ice-cold methanol, and snap frozen (− 80 °C) to prevent further degradation of lipid mediators (see **Supplementary Methods and Methods** for further details). To assess changes in vascular permeability, Evan's blue (100 μl/mouse of a 1% solution in saline) was injected i.p. 24 h prior lung collection. Lungs were fixed with 10% neutral buffered formalin, placed in dimethylformamide (1 ml/g of tissue) and the amount of extravasated dye was quantified on a spectrophotometer using the formula: $Abs_{620nm} - (1.426 - Abs_{740nm} + 0.03)$ as in (ref. 57). BAL total proteins were quantified with the Bradford method.

Lung examination and histology. Lungs excised *en bloc* were inflated with 1 ml of DPBS to permit even organ expansion (critical for quantitative morphometry), fixed, and cut transversally to the trachea into 5, 2 mm thick, parallel slabs/lung starting from the top 2 mm of the lung to ensure uniform random sampling. Slabs were embedded and cut surface-down into 2 μm sections that were stained with H&E or PAS (BioOptica, Milan, Italy) to detect inflammatory cell infiltrates or MuSC. Semi-quantitative scores of lung pathology were assigned on a 0–3 scale, based on criteria described in **Table 1**, minimally modified from (ref. 57). Epithelium thickness (μm) was determined by measuring 15 random fields/lung with the QWin Leica software. Tissue blocks received a numerical code at time of embedding and slides were scored by an investigator blinded to specimen group.

Cell sorting and real time PCR analysis of lung MΦs. Cells obtained upon dissociation of lungs using the GentleMACS dissociator (Miltenyi, Calderara di Reno, Italy) were stained (15 min, 4 °C) with fluorescent anti CD45, EpCAM (CD326), CD11b, F4/80, and CD11c antibodies and sorted using a BD FACS Aria II system. Total RNA and miRNA were isolated with Norgen isolation kits following digestion (18 h, 55 °C) with SDS ($\sim$1%) and proteinase K ($\sim$1 mg) and quantified with a Nanodrop 2000 spectrophotometer and a Quibit 3.0 fluorimeter (Thermo Fisher Scientific, Waltham, MA). RNA was reverse transcribed using the RT^2 PreAMP cDNA Synthesis Kit (SA Biosciences) and loaded into a real time PCR array (SA Biosciences Cat. # PAMM-052Z). For miRNA expression analysis, 1 ng of miRNAs from sorted MΦs was converted into cDNA with the miScript II system (Qiagen, Milan, Italy) and 50 pg of cDNA were used in real time PCR reactions with miScript primers for: mmu-miR-146b-5p (Cat # MS00001645), mmu-miR-155-5p (Cat # MS00001701), mmu-miR-10b-5p (Cat # MS00032249), mmu-miR-21a-5p (Cat # MS00011487) and SNORD61 (Cat # MS00033705) used as a control of equal cDNA input. Reactions were carried out using an ABI 7900 HT thermal cycler and results were analyzed using the $2^{-\Delta Ct}$ method as in (refs 30,33).

Statistics. Results are reported as arithmetic mean ± s.e.m., unless otherwise indicated. Statistical analysis of *in vivo* and *in vitro* experiments was carried out using one-way ANOVA followed by Holm–Sidak or Dunn's *post hoc* test, as appropriate, for the distribution of variance among groups. HPAEC experiments and real time PCR data were analyzed with paired *t*-test. Survival curves and weight loss grade among vehicle- or RvD1-treated infected mice were compared using LogRank Mantel-Cox and χ^2–test, respectively. *P*-values < 0.05 were considered statistically significant.

Study approval. Experimental procedures involving the use of mice were done in accordance with protocols approved by the Ethics Committee of the G. D'Annunzio University of Chieti-Pescara (Protocol #65/2013/CEISA/COM/PROG55).

SUPPLEMENTARY MATERIAL is linked to the online version of the paper at http://www.nature.com/mi

ACKNOWLEDGMENTS

This work was supported in part by the European Union Seventh Framework Programme (FP7/2007–2013) under grant agreement 294187 FP7-PEOPLE-CIG-2011, the Italian Cystic Fibrosis Foundation (FFC#21/2014), the Regione Abruzzo under the Piano Speciale Multiasse Reti per l'Alta Formazione–POFSE 2007–2013, and the Italian Ministry of Health (GR-2011-02349730) (to A.R.). The FFC#21/2014 project was entirely adopted by Unicredit, Iniziativa di Natale FFC 2014, Gruppo di sostegno FFC di Isili (CA), Delegazioni FFC di Soverato (CT), San Costantino Calabro (VV), and Montescaglioso Matera (MT). We thank Alice Rossi, Ida De Fino, and Serena Ranucci for skillful assistance with chronic infection experiments and Sara Di Silvestre for help with HPAEC isolation.

AUTHOR CONTRIBUTIONS

A.R. conceived overall research, designed and carried out experiments, and wrote the full paper; M.C., E.C., A.L., V.C.M., A.N. and M.A. carried out research and analyzed results; A.B. provided expertise on mouse chronic infections; A.B., M.I. and M.R. contributed critical reading of the final version of the manuscript.

DISCLOSURE

The authors declared no conflict of interest.

REFERENCES

1. Pier, G.B. Pseudomonas and Related Gram-Negative Bacillary Infections. In *Goldman's Cecil Med. 24th ed*, 1877–1881 (W.B. Saunders, Philadelphia, PA, 2012).
2. *CDC Office of Infectious Diseases & Centers for Disease Control and Prevention Antibiotic resistance threats in the United States, CDC Threat Rep, Atlanta, GA, 2013.*
3. European Centrefor Disease Prevention and Control *Annual epidemiological report - Antimicrobial resistance surveillance in Europe 2014 Solna, Sweden, 2015.*
4. Bragonzi, A *et al.* Nonmucoid Pseudomonas aeruginosa expresses alginate in the lungs of patients with cystic fibrosis and in a mouse model. *J. Infect. Dis.* **192**, 410–419 (2005).
5. Bragonzi, A. *et al.* Pseudomonas aeruginosa microevolution during cystic fibrosis lung infection establishes clones with adapted virulence. *Am. J. Respir. Crit. Care Med.* **180**, 138–145 (2009).
6. Winstanley, C., O'Brien, S. & Brockhurst, M.A. Pseudomonas aeruginosa evolutionary adaptation and diversification in cystic fibrosis chronic lung infections. *Trends Microbiol.* **24**, 327–337 (2016).
7. Ortega-Gómez, A., Perretti, M. & Soehnlein, O. Resolution of inflammation: an integrated view. *EMBO Mol. Med.* **5**, 661–674 (2013).
8. Serhan, C.N., Hamberg, M. & Samuelsson, B. Lipoxins: novel series of biologically active compounds formed from arachidonic acid in human leukocytes. *Proc. Natl Acad. Sci. USA* **81**, 5335–5339 (1984).
9. Serhan, C.N. *et al.* Novel functional sets of lipid-derived mediators with antiinflammatory actions generated from omega-3 fatty acids via cyclooxygenase 2-nonsteroidal antiinflammatory drugs and transcellular processing. *J. Exp. Med.* **192**, 1197–1204 (2000).
10. Fierro, I.M., Kutok, J.L. & Serhan, C.N. Novel lipid mediator regulators of endothelial cell proliferation and migration: aspirin-triggered-15R-lipoxin A(4) and lipoxin A(4). *J. Pharmacol. Exp. Ther.* **300**, 385–392 (2002).
11. Levy, B.D. *et al.* Protectin D1 is generated in asthma and dampens airway inflammation and hyperresponsiveness. *J. Immunol.* **178**, 496–502 (2007).
12. Serhan, C.N. *et al.* Maresins: novel macrophage mediators with potent antiinflammatory and proresolving actions. *J. Exp. Med.* **206**, 15–23 (2009).
13. Bannenberg, G.L. *et al.* Molecular circuits of resolution: formation and actions of resolvins and protectins. *J. Immunol.* **174**, 4345–4355 (2005).
14. Serhan, C.N. Pro-resolving lipid mediators are leads for resolution physiology. *Nature* **510**, 92–101 (2014).
15. Haworth, O., Cernadas, M., Yang, R., Serhan, C.N. & Levy, B.D. Resolvin E1 regulates interleukin 23, interferon-gamma and lipoxin A4 to promote the resolution of allergic airway inflammation. *Nat. Immunol.* **9**, 873–879 (2008).
16. Norling, L.V. *et al.* Proresolving and cartilage-protective actions of resolvin D1 in inflammatory arthritis. *JCI Insight* **1**, e85922 (2016).
17. Spite, M. *et al.* Resolvin D2 is a potent regulator of leukocytes and controls microbial sepsis. *Nature* **461**, 1287–1291 (2009).
18. Chiang, N. *et al.* Infection regulates pro-resolving mediators that lower antibiotic requirements. *Nature* **484**, 524–528 (2012).
19. Chen, F. *et al.* Resolvin D1 improves survival in experimental sepsis through reducing bacterial load and preventing excessive activation of inflammatory response. *Eur. J. Clin. Microbiol. Infect. Dis.* **33**, 457–464 (2014).
20. Chiang, N., Dalli, J., Colas, R.A. & Serhan, C.N. Identification of resolvin D2 receptor mediating resolution of infections and organ protection. *J. Exp. Med.* **212**, 1203–1217 (2015).
21. Abdulnour, R.E. *et al.* Aspirin-triggered resolvin D1 is produced during self-resolving gram-negative bacterial pneumonia and regulates host immune responses for the resolution of lung inflammation. *Mucosal Immunol.* **9**, 1278–1287 (2016).
22. Croasdell, A., Lacy, S.H., Thatcher, T.H., Sime, P.J. & Phipps, R.P. Resolvin D1 dampens pulmonary inflammation and promotes clearance of nontypeable *Haemophilus influenzae*. *J. Immunol.* **196**, 2742–2752 (2016).
23. Ueda, T. *et al.* Combination therapy of 15-epi-lipoxin A4 with antibiotics protects mice from Escherichia coli-induced sepsis*. *Crit. Care Med.* **42**, e288-95 (2014).
24. Basil, M.C. & Levy, B.D. Specialized pro-resolving mediators: endogenous regulators of infection and inflammation. *Nat. Rev. Immunol.* **16**, 51–67 (2016).
25. Wu, S.-H., Chen, X -Q., Liu, B., Wu, H.-J. & Dong, L. Efficacy and safety of 15(R/S)-methyl-lipoxin A(4) in topical treatment of infantile eczema. *Br. J. Dermatol.* **168**, 172–178 (2013).
26. Fullerton, J.N. & Gilroy, D.W. Resolution of inflammation: a new therapeutic frontier. *Nat. Rev. Drug Discov.* **15**, 551–567 (2016).
27. Serhan, C.N. *et al.* Resolvins: a family of bioactive products of omega-3 fatty acid transformation circuits initiated by aspirin treatment that counter proinflammation signals. *J. Exp. Med.* **196**, 1025–1037 (2002).
28. Sun, Y.-P. *et al.* Resolvin D1 and its aspirin-triggered 17R epimer. Stereochemical assignments, anti-inflammatory properties, and enzymatic inactivation. *J. Biol. Chem.* **282**, 9323–9334 (2007).
29. Norling, L.V., Dalli, J., Flower, R.J., Serhan, C.N. & Perretti, M. Resolvin D1 limits polymorphonuclear leukocyte recruitment to inflammatory loci: receptor-dependent actions. *Arterioscler. Thromb. Vasc. Biol.* **32**, 1970–1978 (2012).
30. Recchiuti, A., Krishnamoorthy, S., Fredman, G., Chiang, N. & Serhan, C.N. MicroRNAs in resolution of acute inflammation: identification of novel resolvin D1-miRNA circuits. *FASEB J.* **25**, 544–560 (2011).
31. Krishnamoorthy, S., Recchiuti, A., Chiang, N., Fredman, G. & Serhan, C.N. Resolvin D1 receptor stereoselectivity and regulation of inflammation and proresolving microRNAs. *Am. J. Pathol.* **180**, 2018–2027 (2012).
32. Krishnamoorthy, S. *et al.* Resolvin D1 binds human phagocytes with evidence for proresolving receptors. *Proc. Natl Acad. Sci. USA* **107**, 1660–1665 (2010).
33. Recchiuti, A. *et al.* Immunoresolving actions of oral resolvin D1 include selective regulation of the transcription machinery in resolution-phase mouse macrophages. *FASEB J.* **28**, 3090–3102 (2014).
34. Schmid, M., Gemperle, C., Rimann, N. & Hersberger, M. Resolvin D1 Polarizes Primary Human Macrophages toward a Proresolution Phenotype through GPR32. *J. Immunol.* **196**, 3429–3437 (2016).
35. Rogerio, A.P. *et al.* Resolvin D1 and aspirin-triggered resolvin D1 promote resolution of allergic airways responses. *J. Immunol.* **189**, 1983–1991 (2012).
36. Wang, B. *et al.* Resolvin D1 protects mice from LPS-induced acute lung injury. *Pulm. Pharmacol. Ther.* **24**, 434–441 (2011).
37. Starke, J.R., Edwards, M.S., Langston, C. & Baker, C.J. A mouse model of chronic pulmonary infection with Pseudomonas aeruginosa and Pseudomonas cepacia. *Pediatr. Res.* **22**, 698–702 (1987).
38. Cigana, C. *et al.* Tracking the immunopathological response to Pseudomonas aeruginosa during respiratory infections. *Sci. Rep.* **6**, 21465 (2016).
39. Pier, G.B. *Pseudomonas* and related gram-negative bacillary infections. *Goldman's Cecil Med,* 24th ed (2012). Q2
40. Alam, M.M. & O'Neill, L.A. MicroRNAs and the resolution phase of inflammation in macrophages. *Eur. J. Immunol.* **41**, 2482–2485 (2011).
41. Bragonzi, A. *et al.* Sequence diversity of the mucABD locus in Pseudomonas aeruginosa isolates from patients with cystic fibrosis. *Microbiology* **152**, 3261–3269 (2006).
42. Samuelsson, B. From studies of biochemical mechanism to novel biological mediators: prostaglandin endoperoxides, thromboxanes, and leukotrienes. Nobel Lecture, 8 December 1982. *Biosci. Rep.* **3**, 791–813 (1983).
43. Frediani, J.K. *et al.* Plasma metabolomics in human pulmonary tuberculosis disease: a pilot study. *PLoS ONE* **9**, e108854 (2014).
44. Flitter, B.A. *et al.* Pseudomonas aeruginosa sabotages the generation of host proresolving lipid mediators. *Proc. Natl Acad. Sci. USA* **114**, 136–141 (2017).
45. Jenner, W. *et al.* Characterisation of leukocytes in a human skin blister model of acute inflammation and resolution. *PLoS ONE* **9**, e89375 (2014).
46. Levy, B.D., Clish, C.B., Schmidt, B., Gronert, K. & Serhan, C.N. Lipid mediator class switching during acute inflammation: signals in resolution. *Nat. Immunol.* **2**, 612–619 (2001).

47. Grassmé, H. *et al.* Regulation of pulmonary Pseudomonas aeruginosa infection by the transcriptional repressor Gfi1. *Cell Microbiol.* **8**, 1096–1105 (2006).
48. Koh, A.Y., Priebe, G.P., Ray, C., Rooijen, N., Van, & Pier, G.B. Inescapable need for neutrophils as mediators of cellular innate immunity to acute pseudomonas aeruginosa pneumonia. *Infect. Immun.* **77**, 5300–5310 (2009).
49. Kim, Y.J. *et al.* Risk factors for mortality in patients with Pseudomonas aeruginosa bacteremia; retrospective study of impact of combination antimicrobial therapy. *BMC Infect. Dis.* **14**, 161 (2014).
50. Konstan, M.W. *et al.* A randomized double blind, placebo controlled phase 2 trial of BIIL 284 BS (an LTB4 receptor antagonist) for the treatment of lung disease in children and adults with cystic fibrosis. *J. Cyst. Fibros.* **13**, 148–155 (2014).
51. Lee, C.G. *et al.* Vascular endothelial growth factor (VEGF) induces remodeling and enhances TH2-mediated sensitization and inflammation in the lung. *Nat. Med.* **10**, 1095–1103 (2004).
52. Lorè, N.I. *et al.* IL-17A impairs host tolerance during airway chronic infection by Pseudomonas aeruginosa. *Sci. Rep.* **6**, 25937 (2016).
53. O'Connell, R.M., Taganov, K.D., Boldin, M.P., Cheng, G. & Baltimore, D. MicroRNA-155 is induced during the macrophage inflammatory response. *Proc. Natl Acad. Sci. USA* **104**, 1604–1609 (2007).
54. Sheedy, F.J. *et al.* Negative regulation of TLR4 via targeting of the proinflammatory tumor suppressor PDCD4 by the microRNA miR-21. *Nat. Immunol.* **11**, 141–147 (2010).
55. Croasdell, A., Sime, P.J. & Phipps, R.P. Resolvin D2 decreases TLR4 expression to mediate resolution in human monocytes. *FASEB J.* **30**, 3181–3193 (2016).
56. Palmer, C.D. *et al.* 17(R)-Resolvin D1 differentially regulates TLR4-mediated responses of primary human macrophages to purified LPS and live E. coli. *J. Leukoc. Biol.* **90**, 459–470 (2011).
57. Matute-Bello, G. *et al.* An Official American Thoracic Society Workshop Report: features and measurements of experimental acute lung injury in animals. *Am. J. Respir. Cell Mol. Biol.* **44**, 725–738 (2011).